Int. J. Electrochem. Sci., 8 **(2013)** 4543 - 4550

International Journal of
ELECTROCHEMICAL
SCIENCE
www.electrochemsci.org

Synthesis of Mesoporous Fe_2O_3 Nanorods and Their Electrochemical Performance

Caihua Wang[1,2], *Linlin Wang*[2] *and Kaibin Tang*[2,*]

[1]School of Chemistry and Chemical Engineering, Fuyang Normal College, Fuyang 236041, P. R. China
[2]Department of Chemistry, University of Science and Technology of China, Hefei 230026, P. R. China
[*]E-mail: chw007@mail.ustc.edu.cn; kbtang@ustc.edu.cn

Received: 6 February 2013 / *Accepted:* 12 March 2013 / *Published:* 1 April 2013

We have successfully prepared mesoporous FeO(OH) nanorods by the solvothermal method using 2-butanone and water mixture solvent for the first time, which are about 30 nm in diameter and 50 nm in length, and it can be converted to mesoporous Fe_2O_3 nanorods via calcination at 300℃. The as-prepared samples were characterized using X-ray diffraction, scanning electron microscopy and transmission electron microscopy. The results showed that the product is mesoporous Fe_2O_3 and some of them are connected. Electrochemical tests demonstrated that the mesoporous Fe_2O_3 nanorods had an initial discharge capacity up to 1187 mA h g-1 and the discharge capacity of 570 mA h g-1 after 50 cycles at 200 mA g-1. After 100 cycles, the discharge capacity is still maintain at 503 mA h g^{-1}.

Keywords: Solvothermal synthesis / Mesoporous Fe_2O_3 / Electrochemical properties

1. INTRODUCTION

Iron oxides are of great scientific and technological importance in fields of catalysts, pigments and gas sensors [1-3]. Among the iron oxides, α- Fe_2O_3, which is the most stable iron oxide with n-type semiconducting properties under ambient conditions, is the most researched and most frequent polymorph in nature as the mineral hematite. Hematite has a rhombohedrally centered hexagonal structure of the corundum type with a close-packed oxygen lattice in which two-thirds of the octahedral sites are occupied by Fe^{3+} ions[4]. Recently, α- Fe_2O_3 has attracted an enormous amount of interest because of its low cost and nontoxicity as an anode material for lithiumion secondary batteries[5-7].

As we know, nanoscale materials often exhibit physical and chemical properties that differ greatly from their bulk counterparts. Various α- Fe_2O_3 with nanostructures have been prepared in recent years, such as nanoparticles[5], nanorods[8], nanotubes[9-10] and flower-like structures[11]. α-Fe_2O_3 hollow spheres were synthesized by a facile quasiemulsion-templated method, which manifested greatly enhanced Li storage properties[12]. α-Fe_2O_3 nanowall arrays grown on Ni foam was advantageous in electron transport and electrolyte diffusion efficiency, which could accelerate the electrochemical reaction[13]. α-Fe_2O_3 dendrites with lengths of 1–4.5 μm along the trunk were synthesized by a low-temperature hydrothermal method and their electrochemical performance as anode material for lithium-ion batteries was also evaluated by charge–discharge measurement[14]. The Fe_2O_3-based thin film electrodes were prepared and exhibited special characteristics regarding the high value of conductivity compared with that of bulk samples[15]. Nanosized α-Fe_2O_3 powders with ca. 50 nm were synthesized via gel polymer route and their capacity was 1300 mA h g-1 at after 200 cycles (0.20 mA/cm2)[16]. In fact, the morphology and particle size of Fe_2O_3 powders had an important influence on the electrochemical performance[17-18]. Moreover, various Fe_2O_3 based materials have been synthesized, such as α-Fe_2O_3 submicro-flowers[19], porous Fe_2O_3 thin films[20], α-Fe_2O_3/C nanocomposite[21], Reduced graphene oxide/Fe_2O_3 composite[22], Fe_2O_3/graphene composite[23] and α-Fe_2O_3/MWCNTs[24], some of which exhibited excellent electrochemical properties.

2. EXPERIMENTAL SECTION

2.1 Materials

Ferric nitrate ($Fe(NO_3)_3 \cdot 9H_2O \geq 99.0$ %), and 2-butanone (C_4H_8O, M_W = 72.11) were purchased from Shanghai Chemical Reagents Co., Ltd. and were used as-received without further purification.

2.2 Synthesis.

In a typical experimental synthesis, 0.1 g of $Fe(NO_3)_3 \cdot 9H_2O$ were dissolved in 3 mL of deionized H_2O under stirring. Then, 37 mL of 2-butanone was added to the above solution. The mixture was stirred for about 10 minutes and then was sealed in a Teflon-lined stainless steel autoclave (50 mL capacity). The autoclave was maintained in an oven at 80 °C for 12 h. The raw products were washed with anhydrous ethanol for three times, and finally dried in a vacuum chamber at 60 °C for 6 h. The obtained precursor was FeOOH. Then it was annealed at 300 °C for 1 h in air atmosphere, the Fe_2O_3 products were obtained.

2.3 Characterization.

The products were characterized by powder X-ray diffraction (XRD) performed on a Philips X'Pert diffractmeter with Cu Kα radiation (λ = 1.54178 Å). Scanning electron microscopy (SEM)

images were taken on a JEOL JSM-6700F scanning electron microscope. Transmission electron microscopy (TEM) images and high-resolution TEM (HRTEM) images were obtained on the JEOL-2010 transmission electron microscope operating at 200 kV. The corresponding selected area electron diffraction (SAED) patterns HRTEM images were taken on a JEOL 2010 high-resolution TEM performing at 200 kV. The samples used for SEM, TEM and HRTEM characterization were dispersed in absolute ethanol and were slightly ultrasonicated before observation.

2.4 Electrochemical measurements.

The electrochemical performance was tested by using coin-type cells (CR2016) at room temperature. The working electrodes were made by mixing the products, acetylene black and polyvinylidene fluoride (PVDF) in N-methylpyrrolidone (NMP) at a weight ratio of 8:1:1. The resulting paste was uniformly coated onto a Cu foil and dried in the vacuum chamber at 100 °C for 10 h, before being cut into disks with a diameter of 8 mm. The coin-type cells were assembled in an glove box under argon atmosphere with the prepared disks as working electrodes, lithium metal as the counter electrodes, microporous membrane (Celgard 2300) as separators and 1M LiPF6 mixed in a solution of ethylene carbonate (EC) and dimethyl carbonate (DMC) (1:1) in volume as electrolyte. The charge–discharge measurements were conducted on a Land CT 2001A automatic battery tester (Wuhan, China).

3. RESULTS AND DISCUSSION

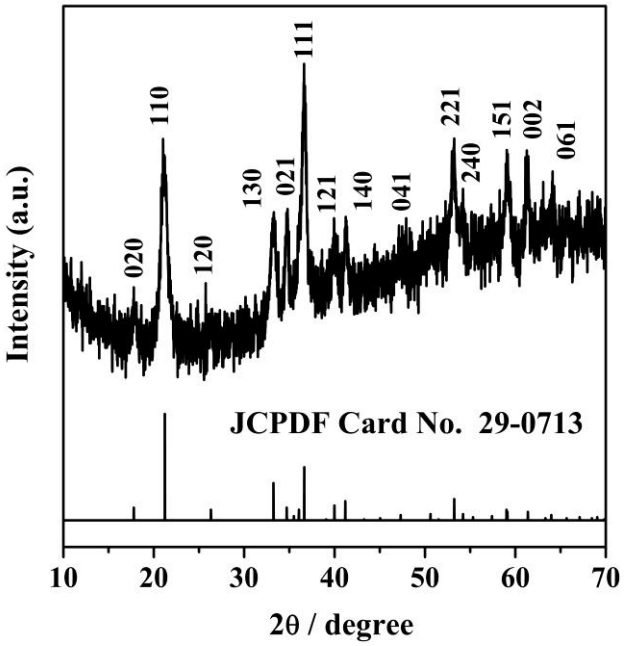

Figure 1. XRD pattern of the prepared FeOOH.

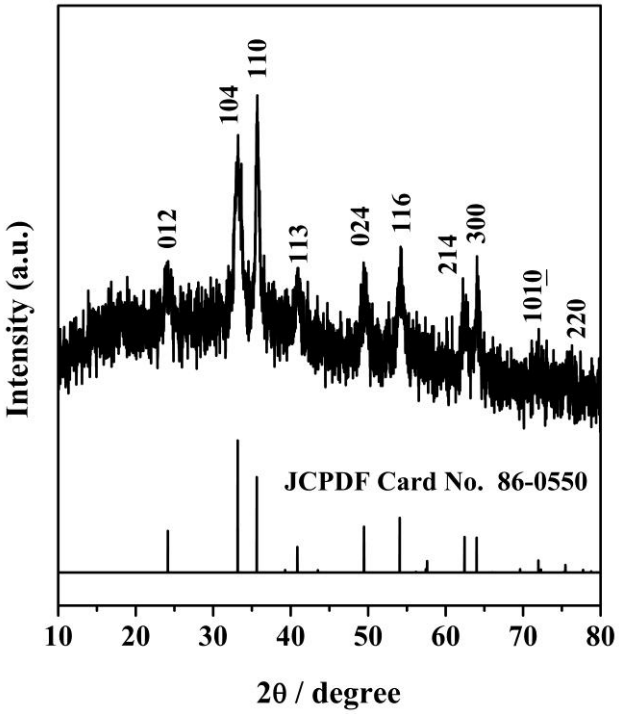

Figure 2. XRD pattern of the mesoporous Fe_2O_3.

The phase purities of FeOOH and Fe_2O_3 were examined by X-ray diffraction. Fig 1 shows the XRD pattern of the typical FeOOH sample, in which all the peaks can be assigned to orthorhombic phase FeOOH (JCPDF Card No. 29-0713, Pbnm). All peaks of the XRD pattern shown in Fig 2 can be indexed to the standard rhombohedral hexagonal phase Fe_2O_3 (JCPDF Card No.86-0550 $R\bar{3}c$), and there are no additional peaks of impurities, indicating that it is pure Fe_2O_3.

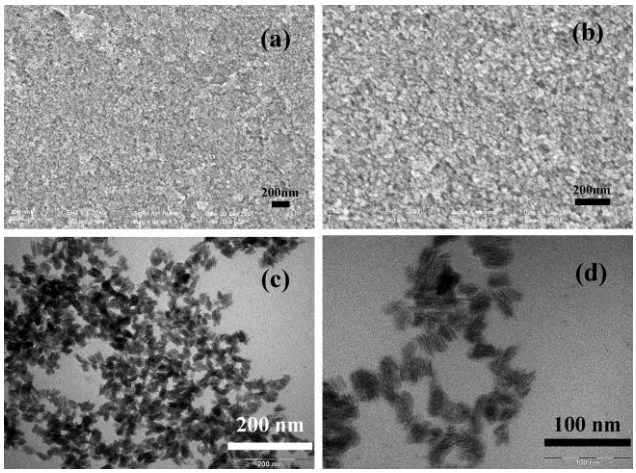

Figure 3. SEM and TEM images of mesoporous FeOOH: (a), (c) Low-magnification SEM and TEM, respectively; (b), (d) high-magnification SEM and TEM.

The morphology of the FeOOH sample has been studied by SEM and TEM. The SEM images are a little unclear because of its too small size, but obviously, the sample is composed of many small nanorods (Fig. 3a and b). From the TEM images (Fig. 3c and d), the FeOOH nanorods are uniformly dispersed. These FeOOH nanorods are about 30 nm in diameter and 50 nm in length, smaller than the reported results[25]. Usually, several nanorods bundle together due to the hydrophobic interaction. It is very surprising that these nanorods possess a uniformly narrow mesoporous structure with an average width of about 2～3 nm.

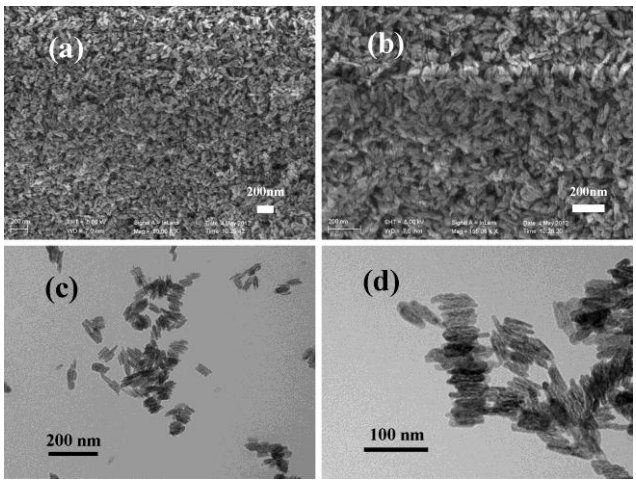

Figure 4. SEM and TEM images of mesoporous Fe_2O_3: (a), (c) Low-magnification SEM and TEM, respectively; (b), (d) high-magnification SEM and TEM.

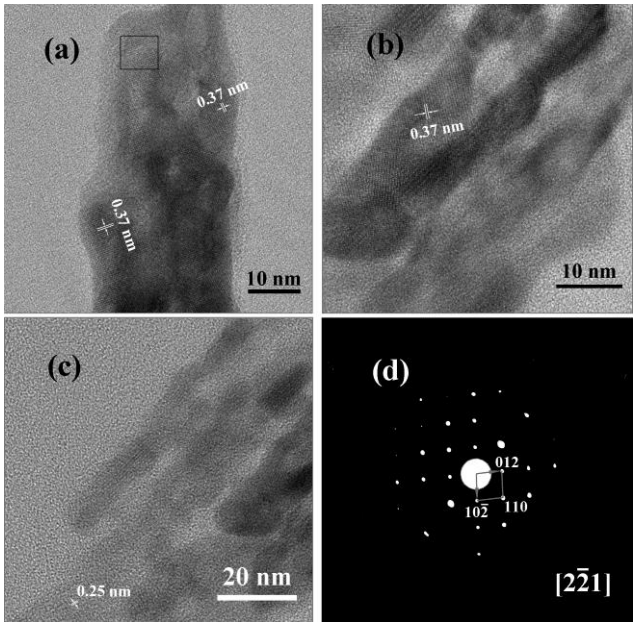

Figure 5. (a-c) HRTEM images of mesoporous Fe_2O_3 nanorods. (d) The corresponding SAED image from the marked part in (a).

Because Fe_2O_3 sample was prepared by annealing the above-mentioned FeOOH, the morphology and microstructure of the Fe_2O_3 sample were researched by SEM and TEM as well, which are shown in Fig 4. It is very easy for us to observe that the Fe_2O_3 sample still reserves its microstructure and size. Comparing with the FeOOH precursor, the mesopores are not completely connected each other.

For further investigating the particular structure of the mesoporous Fe_2O_3 nanorods, the HRTEM images of the typical sample are demonstrated in Fig 5. It can be clearly observed that a lot of mesopores exist in the product, some of which are still connected. The HRTEM image shows resolved lattice fringes of (012) and (110) planes with a spacing of ca. 0.37 and 0.25 nm (Fig 5a-c), consistent with the XRD result. Fig 5d exhibits the SAED pattern taken from the marked part in Fig 5a, which can be indexed to a rhombohedral hexagonal phase (space group $R\bar{3}c$) with lattice constants a = 0.5035 and c = 1.3747 nm.

We evaluated the electrochemical properties of the mesoporous Fe_2O_3 nanorods by a galvanostatic method. The charge-discharge voltage profiles of the Fe_2O_3 sample are shown in Figure 6. A distinct voltage plateau can be clearly identified at ~0.75 V, corresponding to the Li insertion into Fe_2O_3 and the formation of Li_2O, which agrees well with the previous reports[10, 12]. The cycling performance of the sample is depicted in Figure 7 at a constant current density of 200 mA h g^{-1} between 0.05 and 3 V. This reaction provides the dominant contribution to the Li storage capability of the material, giving rise to a high first-cycle discharge capacity of 1187 mA h g^{-1}. The capacity fade of the first cycle is about 8.4%. However, the capacity remain stable at about 570 mA h g^{-1} after 50 cycles, whose capacity retention (48%) approximates to the value of Fe_2O_3 submicro-flowers[11]. After 100 cycles, the discharge capacity is still holding at 503 mA h g^{-1}, which indicates good coulombic efficiency and high specific capacities, compared with the previous reports[11,14,18,]. Furthermore, these values are higher than the capacities of α-Fe_2O_3 microparticles[12].

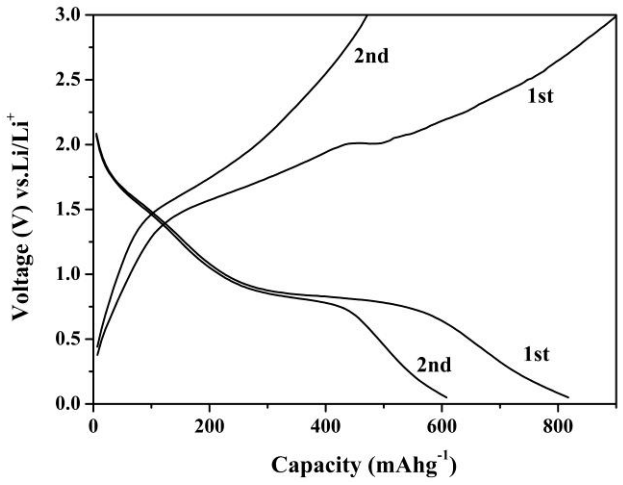

Figure 6. The charge-discharge voltage profiles.

We could also probably attribute this electrochemical performance of the mesoporous materials to its much larger pore size in nanorods, which allow the electrolyte flood completely into the pores and leading to a higher electrolyte/electrode contact area and more facile Li^+ transport in the electrolyte within the pores, and the distinct mesopores interior allowing the material to effectively buffer the stress induced during the charge-discharge process[26-28].

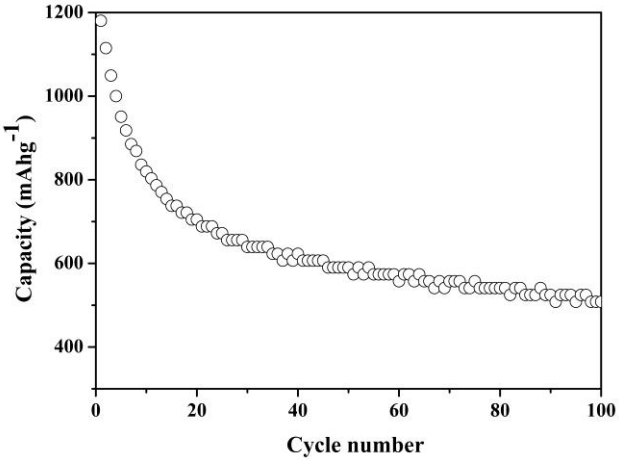

Figure 7. The cycling performance of the mesoporous Fe2O3 nanorods.

4. CONCLUSIONS

In summary, we have successfully prepared mesoporous FeO(OH) nanorods by the solvothermal method using 2-butanone and water mixture solvent for the first time, which are about 30 nm in diameter and 50 nm in length, and it can be converted to mesoporous Fe_2O_3 nanorods via calcination at 300℃ . The created pore size is very small, and some of them are connected. Electrochemical performance of mesoporous Fe_2O_3 nanorods exhibited improved cycling behavior performance and enhanced discharge capacities compared with the electrochemical properties of Fe_2O_3 micoparticles ever reported.

ACKNOWLEDGMENTS
This work was supported by the National Natural Science Foundation of China (No. 91022033, No. 21171158, No. 50903018).

References

1. L. Huo, W. Li, L. Lu, H. Cai, S. Xi, J. Wang, B. Zhao, Y. Shen and Z. Lu, *Chem. Mater.*, 12 (2000) 790
2. M. A. Gondal, A. Hameed, Z. H. Yamani and W. Y. Su, *Chem. Phys. Lett.*, 385 (2004) 111
3. J. S. Han, T. Bredow, D. E. Davey, A. B. Yu and D. E. Mulcahy, *Sensors Actuators B*, 75 (2001) 18

4. R. Zboril, M. Mashlan and D. Petridis, *Chem. Mater.***,** 14 (2002) 969
5. X. Wang, L. Gao, H. Zheng, M. Ji, T. Shen and Z. Zhang, *J. Cryst. Growth*, 269 (2004) 489
6. D. Larcher, C. Masquelier, D. Bonnium, Y. Chabre, V. Masson, J. B. Leriche and J. M. Tarascon, *J. Electrochem. Soc.***,** 150 **(**2003) A133
7. P. Poizot, S. Laruelle, S. Grugeon, L. Dupont and J. M. Tarascon, *Nature*, 407 (2000) 496
8. S. Y. Zeng, K. B. Tang and T. W. Li, *J. Colloid Interface Sci.* 312 (2007) 513
9. J. Chen, L. Xu, W. Y. Li and X. L. Gou, *Adv. Mater.*, 17 (2005) 582
10. J. Chen, L. N. Xu, W. Y. Li and X. L. Gou, *Adv. Mater.*, 17 (2005) 582
11. N. L. Yanna, P. Zhang, Z. P. Guo, P. Munroe and H. K. Liu, *Elctrochim. Acta.*, 53 (2008) 4213
12. B. Wang, J. S. Chen, H. B. Wu, Z, Y, Wang and X, W, Lou, *J. Am. Chem. Soc.*, 133 (2011) 17146
13. D. N. Lei, M. Zhang, B. H. Qu, L. B. Chen, Y. G. Wang, E. D. Zhang, Z. Xu, Q. H. Li and T. H. Wang, *Nanoscale*, 4 (2012) 3422
14. Q. T. Pan, K. Huang, S. B. Ni, F. Yang, S. M. Lin and D. Y. He, *J. Phys. D: Appl. Phys.*, 42 (2009) 015417.
15. J. Sarradina, M. Ribesa, A. Guessousb, K. Elkacemib, *Solid State Ionics*, 112 (1998) 35
16. H. P. Ding, T. Bark, C. H. Chen, *Electrochim. Acta.*, 52 (2007) 6650
17. N. L. Yanna, P. Zhang, Z. P. Guo, H. K. Liu, *J. Electronchem. Soc.*, 155 (2008) A196
18. N. L. Yanna, R. Zeng, P. Zhang, Z. P. Guo, H. K. Liu, *J. Power Sources*, 184 (2008) 456
19. N. L. Yanna, P. Zhang, Z. P. Guo, P. Munroe, H. K. Liu, *Electrochim. Acta.*, 53 (2008) 4213
20. L. Wang, H.W. Xu, P.C. Chen, D.W. Zhang, C.X. Ding, C.H. Chen, *J. Power Sources*, 193 (2009) 846
21. M. F. Hassana, M.M. Rahmana, Z. P. Guo, Z. X. Chen, H. K. Liu, *Electrochim. Acta*, 55 (2010) 5006
22. X. J. Zhu, Y. W. Zhu, S. Murali, M. D. Stollers, R. S. Ruoff, *ACS NANO*, 5 (2001) 3333
23. G. Wang, T. Liu, Y. J. Luo, Y. Zhao, Z. Y. Ren, J. B. Bai, H. Wang, *J. Alloys Compd.*, 509 (2011) L216
24. Y. D. Huang, Z. F. Dong, D. Z. Jia, Z. P. Guo, Solid State Ionics, 201 (2011) 54
25. Z. Y. Zhong, J. Ho, J. Teo, S. C. Shen, A. Gedanken, *Chem. Mater*. 19 (2007) 4776
26. L. L. Wang, H. X. Gong, C. H. Wang, D. K. Wang, K. B. Tang, Y. T. Qian, *Nanoscale*, 4 (2012) 6850
27. Q. Pan, K. Huang, S. Ni, F. Yang, S. Lin, D. He, J. Alloy. Compd., 484 (2009) 322
28. Y. Ren, A. R. Armstrong, F. Jiao, P. G. Bruce, J. Am. Chem. Soc., 132 (2010) 996